European Radiology (2019) 29:3233–3240
https://doi.org/10.1007/s00330-018-5901-5

MUSCULOSKELETAL

High-resolution flat panel CT versus 3-T MR arthrography of the wrist: initial results in vivo

L. Sonnow[1] · S. Koennecker[2] · R. Luketina[2] · T. Werncke[1] · J. B. Hinrichs[1] · B. C. Meyer[1] · F. K. Wacker[1] · C. von Falck[1]

Received: 13 September 2018 / Revised: 25 October 2018 / Accepted: 22 November 2018 / Published online: 14 December 2018

Abstract

Objectives The objective of this study was to compare the diagnostic performance of direct C-arm flat panel computed tomography arthrography (FPCT-A) with direct magnetic resonance arthrography (MR-A) of the wrist in patients with clinically suspected pathologies.

Methods Forty-nine patients underwent tri-compartmental wrist arthrography. FPCT-A was acquired using a high-resolution acquisition mode, followed by a 3-T MR exam using a dedicated wrist coil. Image quality and artifacts of FPCT-A and MR-A were evaluated with regard to the depictability of anatomical structures. The time stamps for the different image acquisitions were recorded for workflow assessment.

Results Image quality was rated significantly superior for all structures for FPCT-A ($p < 0.001$) as compared to MR-A including intrinsic ligaments, TFCC, cartilage, subchondral bone, and trabeculae. The differences in image quality were highest for cartilage (2.0) and lowest for TFCC (0.9). The artifacts were rated lower in MR-A than in FPCT-A ($p < 0.001$). The procedure was more time-efficient in FPCT-A than in MR-A.

Conclusions FPCT-A of the wrist provides superior image quality and optimized workflow as compared to MR-A. Therefore, FPCT-A should be considered in patients scheduled for dedicated imaging of the intrinsic structures of the wrist.

Key Points

- *FPCT arthrography allows high-resolution imaging of the intrinsic wrist structures.*
- *The image quality is superior as compared to MR arthrography.*
- *The procedure is more time-efficient than MR arthrography.*

Keywords Radiology · Joint · Wrist · Arthrography

Abbreviations

DAP	Dose-area product
DRUJ	Distal radioulnar joint
FOV	Field of view
FPCT	Flat panel computed tomography
MDCT	Multidetector computed tomography
MJ	Midcarpal joint
MRA	Magnetic resonance arthrography
MRI	Magnetic resonance imaging
LTL	Lunotriquetral ligament
PDw	Proton density weighted
RC	Radiocarpal joint
SLL	Scapholunate ligament
TE	Echo time
TFCC	Triangular fibrocartilage complex
TR	Repetition time
TSE	Turbo spin echo

✉ L. Sonnow
sonnow.lena@mh-hannover.de

[1] Department of Diagnostic and Interventional Radiology, Medical School Hannover, Carl-Neuberg-Str. 1, 30625 Hannover, Germany

[2] Department of Plastic, Hand and Reconstructive Surgery, Medical School Hannover, Carl-Neuberg-Str. 1, 30625 Hannover, Germany

Introduction

Complex wrist injuries are often associated with soft tissue damage that may lead to chronic wrist pain, long-term arthritic changes, and disability [1, 2]. Standard magnetic resonance imaging (MRI) without intravenous or intra-articular contrast is regarded the first-line cross-sectional imaging modality in

patients with chronic wrist pain as it may reveal a broad spectrum of underlying diseases. However, the diagnostic accuracy of MRI with respect to the depiction of intra-articular structures is limited in subacute cases without traumatic joint effusion. Direct magnetic resonance arthrography (MR-A) adds to the accuracy when compared to conventional MRI [3] and should therefore be considered in cases where standard MRI is equivocal and intrinsic ligament or TFCC tear is clinically suspected. Magee et al could detect ligament and triangular fibrocartilage complex (TFCC) tears in MRA with a sensitivity of 100% [3]. In a systematic review and meta-analysis, Smith et al reported about a pooled sensitivity of 75% for TFCC tears in MRI and 84% in MR-A [4]. Even recent studies with microscopy coils show a limited sensitivity for MR as compared with MR-A [5].

Multidetector computed tomography (MDCT) is a competing diagnostic modality, which is routinely performed for direct MDCT arthrography (MDCT-A) of joints using intra-articular injection of (diluted) iodinated contrast medium. It is considered as accurate as or even more accurate than MR-A for detecting intrinsic ligament and TFCC tears [6, 7]. Recent detector designs result in a maximal z-resolution of 0.4 to 0.5 mm and allow the detection of small defects in bone or cartilage surface. Improvements in MDCT performance such as reduction of metal artifacts and its wide availability make it valuable in clinical routine [8, 9].

Flat panel computed tomography (FPCT) is a relatively new imaging modality which has the potential to outperform MDCT-A based on its superior spatial resolution. Flat panel detectors consist of structured cesium iodide scintillator crystals and provide submillimeter isotropic voxel sizes, which results in an approximately 3-fold higher z-resolution compared to MDCT [10]. FPCT is usually part of an angiography unit and therefore facilitates both fluoroscopic guided contrast agent injection and cross-sectional arthrography in a single examination, thereby optimizing workflow by eliminating the need of a patient transfer. In recent studies, Guggenberger et al showed FPCT-A being as feasible as CT-A and allowing similar image quality [10, 11]. However, these studies were first experiences on phantoms and human cadavers without evaluation of FPCT-A in vivo.

Therefore, the objective of this study was to evaluate the feasibility and performance of FPCT-A in comparison to 3-T MR-A in patients with clinically suspected wrist pathologies. Moreover, we aimed at analyzing the possible workflow optimization of the "one-stop-shop" approach.

Materials and methods

Patient data

The retrospective analysis was approved by the Institutional Ethics Committee and waiver of informed consent was given. The combination of MR and (FP) CT arthrography is a standard procedure in our institution. Between August 2013 and January 2016, a total of 50 wrist arthrographies were performed in 49 patients (28 men, 21 women, mean age 40 years, range 16–70 years) that had been referred by the Department of Plastic, Hand and Reconstructive Surgery. Thirty of the 50 patients had sustained acute trauma resulting in chronic wrist pain and the remaining 19 patients had chronic wrist pain of unknown cause. Indications for direct arthrography were suspicion of intrinsic ligament tear or TFCC pathology based on clinical findings or equivocal standard non-contrast MRI. Detailed patient characteristics are given in Table 1.

Contrast application

After having obtained informed consent, the patient was placed supine in the "superman position" on the examination table of a ceiling-mounted angiography system (Artis Q, Siemens Healthineers). Afterward, tri-compartmental injection into the distal radioulnar (DRUJ), the midcarpal joint (MC), and the radiocarpal joint (RC) was performed under sterile conditions, local anesthesia (Prilocaine 1%, Xylonest® 1%, Astra Zeneca), and fluoroscopic guidance using a 25-G needle. The contrast agent consisted of a 2:3 mixture of an iodinated contrast agent (Iomeprol 300 mg/ml, Imeron 300, Bracco Imaging) and a pre-diluted gadolinium-based contrast agent (Gadolinium-DTPA 2 mmol/l, Magnevist 2 mmol/l, Bayer Vital GmbH). After injection, the wrist was passively moved and gentle traction was applied to ensure a distension and homogenous distribution of the contrast agent within the joint.

Table 1 Patient characteristics

	Number of patients
Indication	
Suspected ligament tear (SLL/LTL)	25
Suspected TFCC lesion	27
Suspected cartilage pathology	7
Unspecific pain	9
Other (edema, inflammation, nonunion)	10
Diagnosis	
SLL tear (partial or complete)	17
LTL tear (partial or complete)	7
TFCC lesion	19
Chondral defect	7
Aseptic osteonecrosis of the lunate	4
Degenerative deformity	4
No pathology	8
Other	11

Image acquisition and postprocessing

Immediately after intra-articular injection, FPCT-A was acquired on the same angiographic system with the C-arm-mounted FP detector operating in a high-resolution 1 × 1 readout mode ("DynaCT micro ®") as shown in detail in Table 2. Tube voltage was set to 109 kVp and the automatic exposure control was applied. Images were reconstructed using the smallest possible volume-of-interest per patient using the "normal" reconstruction kernel. The subsequently resulting voxel size was in the range of 0.11–0.12 mm.

MR images were acquired directly after the immediate transfer to the MR suite using a 3-T MR scanner (MAGNETOM Verio, Siemens Healthineers) and a dedicated 8-channel phase array wrist coil with the patient positioned in "superman" position. The image protocol comprised PD- and T1-weighted Turbo Spin Echo (TSE) sequences with spectral fat suppression in three planes and an isotropic 3D Turbo Spin Echo sequence (SPACE). The scan parameters are given in detail in Table 3. To assess the time between intra-articular injection and FPCT, and FPCT and MR imaging, the time stamps of the last fluoroscopic image of FPCT and first MR sequence were noted.

Image assessment

Two blinded radiologists with 3 and 10 years of experience in reading musculoskeletal images evaluated all FPCT-A and MR-A images independently on a client-server–based PACS workstation (Visage 7.1, Visage Imaging GmbH) using a 5-point Likert scale. Evaluation included the assessment of the following anatomical structures: scapholunate ligament (SLL), lunotriquetral ligament (LTL), TFCC, cartilage of the RC joint, subchondral bone, and trabecular structure. The readers were encouraged to use the 3D functionality of the review software such as multiplanar reformations and thin slab averaging. The 5-point Likert scale was used for evaluation of image quality of the anatomical structure as follows: 1 = excellent image quality, 2 = good image quality, 3 = satisfactory image quality, 4 = poor image quality, 5 = insufficient image quality. Image artifacts were evaluated using the following scale: 1 = no artifacts, 2 = minimal artifacts, 3 = considerable artifacts, 4 = artifacts impairing diagnostic validity, 5 = no interpretation possible.

Table 2 Scan parameters of the FPCT/DynaCT micro (Q Artis Siemens)

Binning mode	1 × 1
Scan duration	20 s
Tube voltage	109 kV
Tube current	55–135 mA
Field of view (FOV)	22 cm
Average dose-area product (DAP)	337.02 μGym^2

Statistical analysis

All statistical analyses were calculated with SPSS Statistics 22.0 (IBM Corp.) and R Version 3.2.4 [12].

Interreader agreement for FPCT-A and MR-A was calculated using Cohen's kappa for the assessment of image quality of all anatomical structures and image artifacts, respectively. In addition, a Cohen's Kappa with quadratic weights was applied in order to distinguish between minor and major disagreement. The Kappa values were interpreted as follows: values ≤ 0 as indicating no agreement, 0.01–0.20 as none to slight, 0.21–0.41 as fair, 0.41–0.60 as moderate, 0.61–0.80 as substantial, and 0.81–1.00 as almost perfect agreement [13].

Image quality for each anatomical structure and imaging modality was compared between FPCT-A and MR-A using the non-parametric Wilcoxon test for dependent samples. A p value lower than 0.05 was considered statistically significant.

Results

The summarized interreader agreement for all anatomical structures showed a substantial agreement for FPCT-A (weighted 0.67/unweighted 0.60) and a substantial agreement (0.72 weighted/0.61 unweighted) for MR-A.

Interreader agreement of image artifacts was moderate to substantial for FPCT-A (weighted 0.72/unweighted 0.53), and substantial to almost perfect for MR-A (weighted 0.83/unweighted 0.62), respectively. Due to the substantial to almost perfect interreader agreement of the ratings, also a mean value was calculated and used for statistical evaluation. Figure 1 illustrates typical FPCT-A images in the coronal and axial reformation together with the corresponding MR-A images as typically evaluated by the readers.

For each anatomical structure, the depictability was rated significantly ($p < 0.001$) superior for FPCT-A as compared to MR-A. Largest differences of image quality were observed for cartilage (1.4 ± 0.6), trabeculae (1.1 ± 0.3), and subchondral bone (1.2 ± 0.5) in FPCT-A compared to MR-A with values of 3.4 ± 0.5, 3.0 ± 0.2, and 3.0 ± 0.3, respectively. The difference in image quality was lowest for the TFCC. Details are given in Table 4. Image artifacts were not statically significant between both image modalities. The artifacts in FPCT were predominantly ring and stripe artifacts. The MR artifacts had a higher variance and were mostly attributed to susceptibility artifacts in cases of osteosynthesis or motion artifacts. Figure 2 illustrates typical examples of common wrist pathologies in FPCT-A and MR-A. Figure 3 summarizes the average image quality grading by both readers for different anatomical structures.

Table 3 Scan parameters of the 3-T MRA (Verio Siemens)

Sequence	TR (ms)	TE (ms)	Flip angle (°)	Bandwidth (Hz/pix)	Slice thickness (mm)	Slice spacing (mm)	FOV (mm)
PD TSE (fs) coronal	5350	39	150	85	2	2.2	130 × 129
T1 TSE (fs) coronal	877	32	145	233	2	2.2	88 × 110
T1 TSE (fs) axial	694	30	145	233	2	2.2	150 × 121
T1 TSE sagittal	976	32	145	233	2	2.2	77 × 110
PD spc rst (fs) coronal	1000	45	120	460	0.6	0.6	110 × 157

The mean time between the last fluoroscopic image and FPCT images was 4 ± 2 min (mean ± standard deviation). The MR scan was acquired on average 67 ± 27 min after the end of the FPCT acquisition.

Discussion

While standard non-contrast MRI is regarded the first-line modality in patients with chronic wrist pain, it is well known

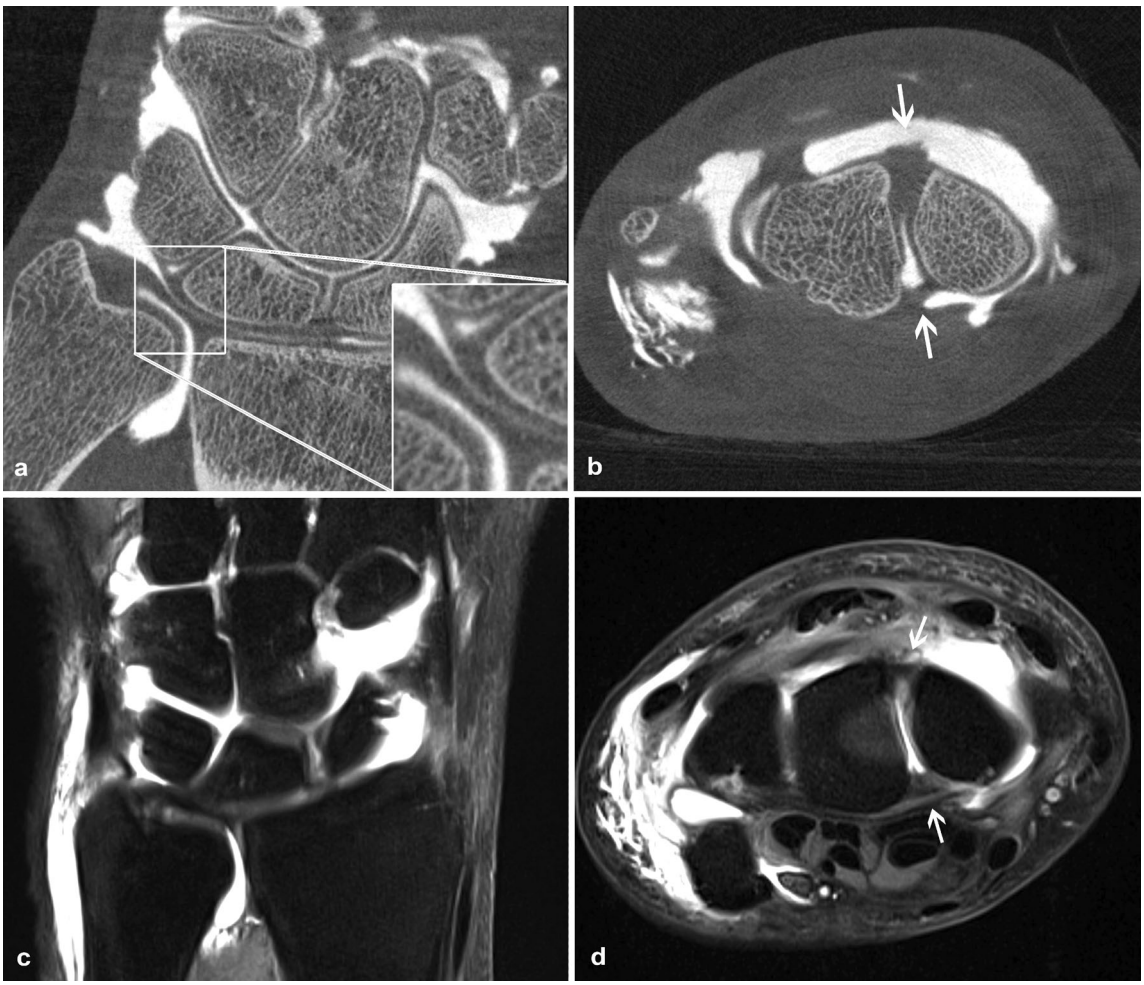

Fig. 1 Coronal (**a**) and axial (**b**) reconstruction of an FPCT-A illustrating anatomical structures like TFCC, LTL, dorsal (upper arrow) and volar (lower arrow) parts of the SLL, cartilage, subchondral bone layer, and trabeculae. All three articular compartments are adequately filled. The high spatial resolution allows a clear depiction of trabeculae and the subchondral bone layer. In the center of the image, typical ring artifacts and predominantly in the periphery of the image beam hardening artifacts become visible. The image quality of this scan was assessed as "excellent" and the artifact extent as "minimal" by both readers. PD TSE coronal (**c**) and T1 TSE axial (**d**) fat saturated sequences of an MR-A illustrating anatomical structures like TFCC, LTL, dorsal (upper arrow) and volar (lower arrow) parts of the SLL, and cartilage. The contrast agent is similarly adequately distributed in all three articular compartments. In comparison to the FPCT-A, the borders of the anatomical structures appear slightly more blurred leading to the assessment of the image quality as "good" for the TFCC, SLL, and LTL as well as "satisfactory" for cartilage, subchondral bone, and trabeculae by both readers. The artifacts were rated as "no artifacts"

Table 4 Mean image quality for each imaging modality, reader, and anatomical structure

Image quality	FPCT-A			MR-A			*p* value
	Reader 1	Reader 2	Mean reader 1 + 2	Reader 1	Reader 2	Mean reader 1 + 2	
SLL	1.2 ± 0.5	1.2 ± 0.5	1.2 ± 0.5	2.7 ± 0.6	2.7 ± 0.7	2.6 ± 0.7	< 0.001
LTL	1.2 ± 0.5	1.2 ± 0.5	1.2 ± 0.5	2.7 ± 0,6	2,9 ± 0.7	2.8 ± 0.7	< 0.001
TFCC	1.2 ± 0.4	1.1 ± 0.3	1.2 ± 0.4	2.4 ± 0.7	1.9 ± 0.8	2.1 ± 0.8	< 0.001
Cartilage	1.4 ± 0.6	1.3 ± 0.5	1.4 ± 0.6	3.4 ± 0.5	3.3 ± 0.5	3.4 ± 0.5	< 0.001
Subchondral bone	1.2 ± 0.5	1.2 ± 0.5	1.2 ± 0.5	3.0 ± 0.4	3.0 ± 0.3	3.0 ± 0.3	< 0.001
Trabeculae	1.1 ± 0.3	1.0 ± 0.1	1.1 ± 0.3	3.0 ± 0.3	3.0 ± 0.2	3.0 ± 0.2	< 0.001
Artifacts	2.1 ± 0.7	2.0 ± 1.0	2.1 ± 0.7	2.0 ± 1.0	1.8 ± 1.0	2.0 ± 1.1	< 0.001

Values are given in mean ± standard deviation. The *p* value given for the comparison of the mean value of both readers between both image modalities

that with respect to imaging of the intrinsic structures of the wrist, the assessment of SLL, LTL, and TFCC integrity is challenging due to their small size and variable appearance [14]. Lee et al showed in a cadaver study that CT and MR arthrography have a very high degree of accuracy for diagnosing tears of the SLL, LTL, and TFCC with both being more accurate than conventional MR imaging [15]. In analogy, the superiority of MDCT arthrography over MRI was verified in studies with other joints; e.g., it was more precise at showing fissures and grading lesions of patellar cartilage [16] and more accurate than 3D MR sequences for measurement of articular cartilage thickness in the ankle [17].

In our study, we compared two arthrographic imaging techniques for the depiction of intrinsic structures of the wrist. We found that FPCT-A was rated significantly better when compared with MR-A with regard to depiction of anatomical structures. These results are in line with previous MDCT-A studies. MDCT-A had a higher specificity than MR-A for the detection of labral pathology of the hip [18] and it showed better accuracy than did MR-A in the detection of osseous, cartilage, and labroligamentous injuries related to anterior shoulder instability [19]. Similarly, in the study of Lee et al, the performance of MDCT-A of the wrist was marginally better than that of MR-A [15]. Moser et al compared MDCT-A and MR-A of the wrist and concluded MDCT-A being beneficial for the diagnosis of partial SLL and LTL tears, cartilage abnormalities, and subtle bone avulsions, mostly owing to its superior spatial resolution and the possibility to interactively generate high-quality multiplanar reformations adjusted to the different anatomical structures [6]. Recent publications also describe a beneficial effect of 3D sequences in MR-A with respect to the depiction of small structures of the wrist as compared to standard 2D imaging [20]. Isotropic 3D MR imaging enables high-quality multiplanar reformations that are crucial for the exact depiction of small anatomical structures of interest that are usually not aligned to the standard imaging planes. However, in our study, FPCT-A was still rated superior as compared to an isotropic submillimeter 3D sequence which is part of our standard MR-A protocol, as described above.

FPCT-A was first described by Guggenberger et al Their experimental studies demonstrated superiority of the flat panel detector CT over MDCT-A. The authors found that in vitro FPCT-A of artificial joint phantoms offers superior contrast-to-noise ratios and artificial cartilage defect depiction quality as compared to MDCT [21]. In phantom and animal studies, FPCT-A showed similar or superior image quality and anatomic depiction of bone, cartilage, and soft tissue compared to standard MDCT-A [9]. With regard to the effective radiation dose, the results of a phantom and cadaveric study indicate that FPCT of the wrist with the patient in the standard "superman" position and using a 1 × 1 binning mode has a comparably low radiation dose as MDCT [22]. First experiences with FPCT-A in human cadaveric wrist joints described similar image quality, but remarkably exceeding contrast-to-noise ratio of FPCT as compared to standard MDCT [11]. Similarly, Chemouni et al showed FPCT-A being accurate for detecting cartilage defects in the cadaveric ankle joint and therefore being an alternative to MDCT-A [23]. To the best of our knowledge, our study is the first experience of using FPCT-A in vivo.

There are certain pathologies in patients with wrist pain, which can be visualized by MRI, only. These include bone marrow edema, osteonecrosis, and inflammatory changes like synovitis. Moser et al describe a better contrast resolution of MR-A that is useful for bone marrow and soft tissue assessment, suggesting a potential advantage or MR-A over MDCT-A [6]. It is important to consider, however, that although the abovementioned diagnoses bear a high clinical importance, all of them can be detected by a conventional MRI without intra-articular contrast injection. Following the American College of Radiology (ACR)-Appropriateness Criteria (last review date 2012), an MRI of the wrist without contrast is the recommended diagnostic modality in case of chronic wrist pain after plain radiographs. Consequently, direct cross-sectional arthrography of the wrist is an invasive procedure that should be only

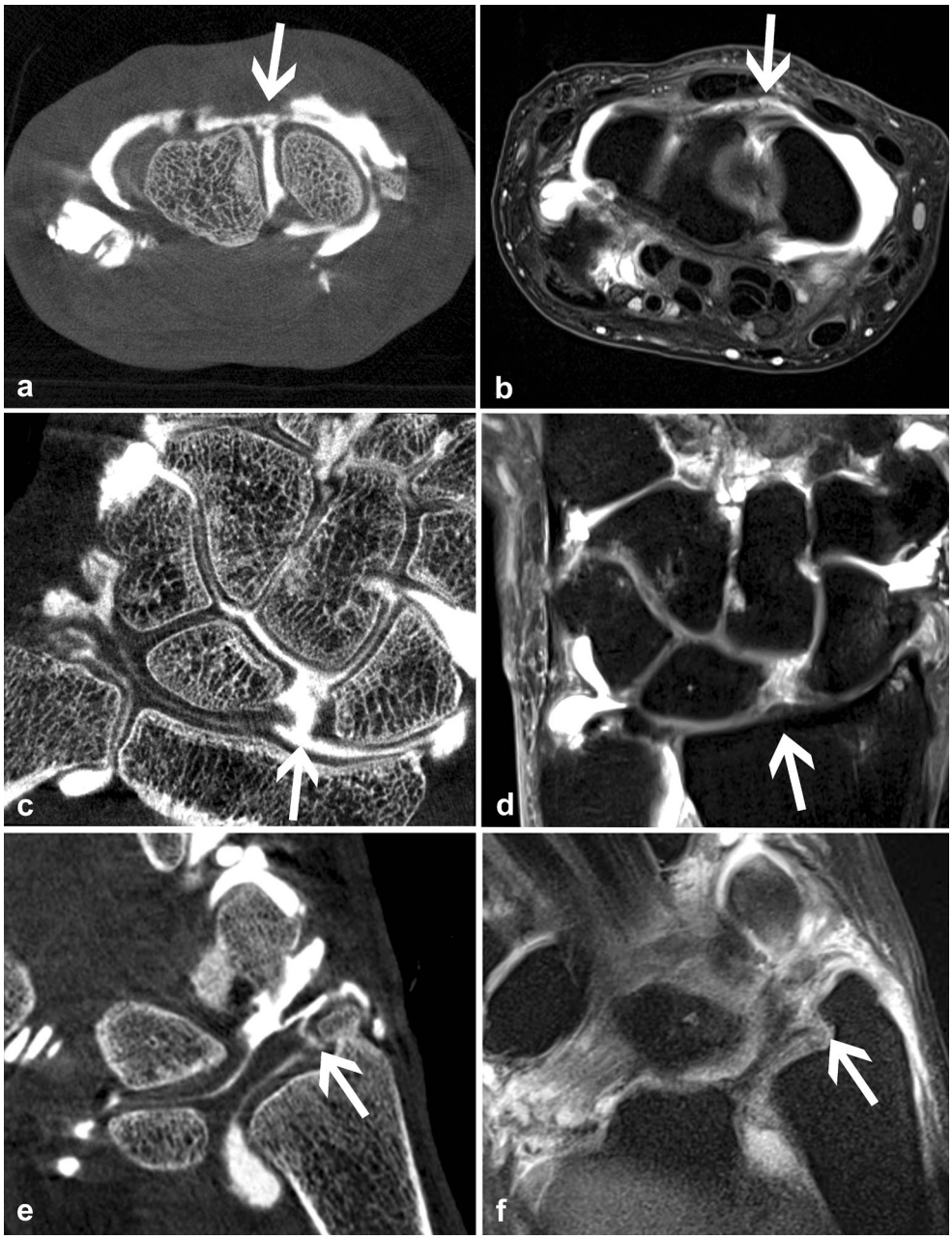

Fig. 2 Common wrist pathologies in FPCT-A vs. MR-A (T1 TSE FS axial and PD TSE FS coronal): A rupture of the dorsal part of the SLL (**a**, **b**) as well as of the membranous SLL (**c**, **d**) can be directly visualized in FPCT-A, whereas in MR-A, the pathology becomes less obvious as thickening and signal increase of the ligament. Similarly, an ulnar TFCC tear can be depicted in FPCT-A and only be suspected in the corresponding MR-A (**e**, **f**)

considered when intrinsic ligament or TFCC injury is clinically suspected and/or standard MRI shows equivocal findings. In these cases, MR-A does not provide new additional information as compared with CT-A. In contrast, CT-A can even give additional insights into the joint by providing detailed information about the cartilage and the subchondral bone plate.

Besides excellent image quality, a major advantage of FPCT is the optimized workflow. FPCT can be acquired immediately after contrast agent injection on the same C-arm CT unit without any delay, e.g., due to patient transfer. In addition, motion artifacts due to a long scan time are minimal and problems with patients who are not or partly suitable for MR (patients with implanted electronic devices or claustrophobic patients) can be avoided.

A potential shortcoming of the FPCT is the occurrence of artifacts, which were rated higher with FPCT-A than with MR-A in our study. As these artifacts can mostly be attributed to technical challenges of FPCT, there is potential for an optimized image quality with the further development of FPCT reconstruction. Personal experience shows that an accurate and frequent calibration of the imaging unit helps to minimize these artifacts. It is also important to mention that the quality of the FPCT scan significantly depends on an adequate distribution of the contrast agent in all three joint compartments. Consequently, if a proper intra-articular contrast agent application is impossible, an MRI scan should be preferred as it depicts pathologies of the intrinsic structures of the wrist (with a limited sensitivity) in

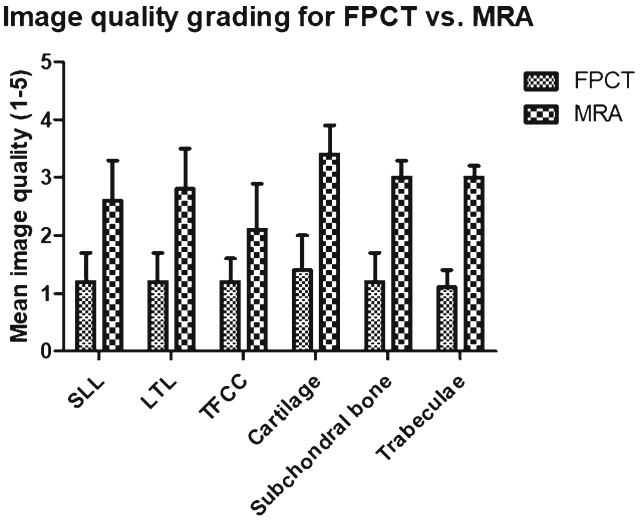

Fig. 3 Average image quality grading for each anatomical structure and modality by both readers

non-contrast or limited contrast scans. Another limitation of our study design is the lack of comparison to a diagnostic arthroscopy. In our study, only 14 of the patients received a subsequent arthroscopy, which is insufficient for an appropriate statistical analysis. This is due to the retrospective nature of this study, as invasive procedures such as arthroscopy or open surgery were indicated by a comprehensive clinical assessment rather than in a standardized prospective study setting.

In conclusion, in our study, FPCT-A of the wrist was advantageous over MR-A regarding the depictability of the intrinsic ligaments, the TFCC, and the cartilage. With regard to workflow aspects, the FPCT-A is a very fast and comfortable diagnostic modality by combining fluoroscopy and cross-sectional imaging in a single modality. Therefore, FPCT-A should be seriously considered as a possible alternative to MR-A in patients scheduled for dedicated imaging of the intrinsic structures of the wrist.

Funding The authors state that this work has not received any funding.

Compliance with ethical standards

Guarantor The scientific guarantor of this publication is PD Dr. von Falck.

Conflict of interest The authors of this manuscript declare no relationships with any companies, whose products or services may be related to the subject matter of the article.

Statistics and biometry One of the authors has significant statistical expertise. No complex statistical methods were necessary for this paper.

Informed consent Written informed consent was obtained from all subjects (patients) in this study.

Ethical approval Institutional Review Board approval was obtained.

Methodology
- retrospective
- observational
- performed at one institution

References

1. Kümmel A, Ebner L, Kraus M et al (2014) Magnet resonance imaging in common injuries of the wrist. Unfallchirurg 117:221–226
2. Rohman EM, Agel J, Putnam MD, Adams JE (2014) Scapholunate interosseous ligament injuries: a retrospective review of treatment and outcomes in 82 wrists. J Hand Surg Am 39:2020–2026
3. Magee T (2009) Comparison of 3-T MRI and arthroscopy of intrinsic wrist ligament and TFCC tears. AJR Am J Roentgenol 192:80–85
4. Smith TO, Drew B, Toms AP, Jerosch-Herold C, Chojnowski AJ (2012) Diagnostic accuracy of magnetic resonance imaging and magnetic resonance arthrography for triangular fibrocartilaginous complex injury: a systematic review and meta-analysis. J Bone Joint Surg Am 94:824–832
5. Štouračová A, Šprláková-Puková A, Čižmář I, Procházková J, Janoušová E, Vališ P (2016) High-resolution MR examination of the scapholunate ligament using a microscopic coil: comparison with direct MR arthrography and arthroscopy findings. Acta Chir Orthop Traumatol Cech 83:327–331
6. Moser T, Dosch JC, Moussaoui A, Dietemann JL (2007) Wrist ligament tears: evaluation of MRI and combined MDCT and MR arthrography. AJR Am J Roentgenol 188:1278–1286
7. Schmid MR, Schertler T, Pfirrmann CW et al (2005) Interosseous ligament tears of the wrist: comparison of multi-detector row CT arthrography and MR imaging. Radiology 237:1008–1013
8. Fischer W, Bohndorf K, Kreitner KF, Schmitt R, Wörtler K, Zentner J (2009) Indications for CT and MR arthrography–recommendations of the musculoskeletal workgroup of the DRG. Rofo 181:441–446
9. Guggenberger R, Fischer MA, Hodler J, Pfammatter T, Andreisek G (2012) Flat-panel CT arthrography: feasibility study and comparison to multidetector CT arthrography. Invest Radiol 47:312–318
10. Kyriakou Y, Struffert T, Dörfler A, Kalender WA (2009) Basic principles of flat detector computed tomography (FD-CT). Radiologe 49:811–819
11. Guggenberger R, Morsbach F, Alkadhi H et al (2013) C-arm flat-panel CT arthrography of the wrist and elbow: first experiences in human cadavers. Skeletal Radiol 42:419–429
12. irr: Various coefficients of interrater reliability and agreement version 0.84 from CRAN. https://rdrr.io/cran/irr/. Accessed 21 Oct 2018
13. McHugh ML (2012) Interrater reliability: the kappa statistic. Biochem Med (Zagreb) 22:276–282
14. Robinson G, Chung T, Finlay K, Friedman L (2006) Axial oblique MR imaging of the intrinsic ligaments of the wrist: initial experience. Skeletal Radiol 35:765–773
15. Lee RK, Ng AW, Tong CS et al (2013) Intrinsic ligament and triangular fibrocartilage complex tears of the wrist: comparison of MDCT arthrography, conventional 3-T MRI, and MR arthrography. Skeletal Radiol 42:1277–1285
16. Daenen BR, Ferrara MA, Marcelis S, Dondelinger RF (1998) Evaluation of patellar cartilage surface lesions: comparison of CT arthrography and fat-suppressed FLASH 3D MR imaging. Eur Radiol 8:981–985
17. El-Khoury GY, Alliman KJ, Lundberg HJ, Rudert MJ, Brown TD, Saltzman CL (2004) Cartilage thickness in cadaveric ankles: measurement with double-contrast multi-detector row CT arthrography versus MR imaging. Radiology 233:768–773
18. Sahin M, Calisir C, Omeroglu H, Inan U, Mutlu F, Kaya T (2014) Evaluation of labral pathology and hip articular cartilage in patients

with femoroacetabular impingement (FAI): comparison of multidetector CT arthrography and MR arthrography. Pol J Radiol 79:374–380

19. Acid S, Le Corroller T, Aswad R, Pauly V, Champsaur P (2012) Preoperative imaging of anterior shoulder instability: diagnostic effectiveness of MDCT arthrography and comparison with MR arthrography and arthroscopy. AJR Am J Roentgenol 198:661–667
20. Sutherland JK, Nozaki T, Kaneko Y et al (2016) Initial experience with 3D isotropic high-resolution 3 T MR arthrography of the wrist. BMC Musculoskelet Disord 17:30. https://doi.org/10.1186/s12891-016-0890-5
21. Guggenberger R, Winklhofer S, Spiczak JV, Andreisek G, Alkadhi H (2013) In vitro high-resolution flat-panel computed tomographic arthrography for artificial cartilage defect detection: comparison with multidetector computed tomography. Invest Radiol 48:614–621
22. Werncke T, Sonnow L, Meyer BC et al (2017) Ultra-high resolution C-arm CT arthrography of the wrist: radiation dose and image quality compared to conventional multidetector computed tomography. Eur J Radiol 89:191–199
23. Chemouni D, Champsaur P, Guenoun D, Desrousseaux J, Pauly V, Le Corroller T (2014) Diagnostic performance of flat-panel CT arthrography for cartilage defect detection in the ankle joint: comparison with MDCT arthrography with gross anatomy as the reference standard. AJR Am J Roentgenol 203:1069–1074